VI. Magnetism in Small Structures

(1) Introduction

(2) Exchange Coupling

(3) Nanostructured Magnetic Materials

(4) Surface and Thin Film Magnetism

(1) INTRODUCTION

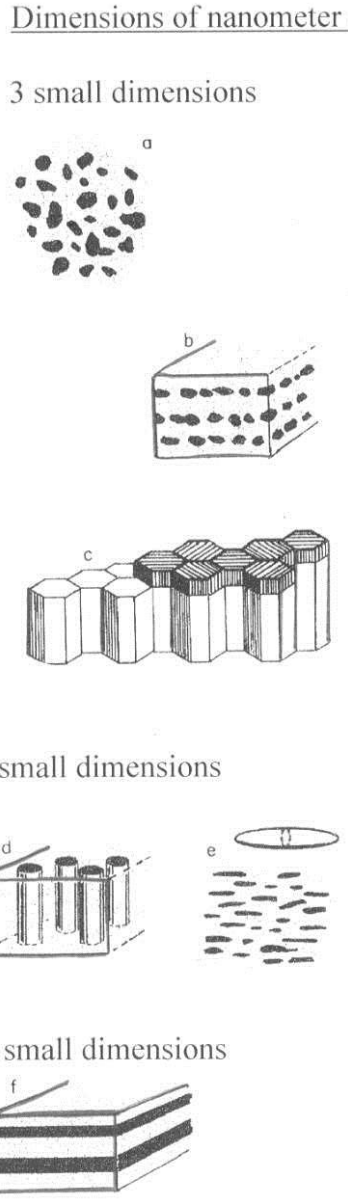

▶ Nanostructured Magnetic Materials

(a) Granular solids in which one or both phases are magnetic

Single-domain crystalline particles in an amorphous matrix:

- Fe-B-Si-Nb-Cu: Fe_3Si particles in a matrix of residual amorphous phase
- Co-Nb-B: Co_nB particles in a nonmagnetic amorphous Nb-B-rich matrix, - $(Fe\text{-}Co)_{80}M_9C_{10}$,

Composite nanostructured permanent magnets: α-Fe/Fe-Nd-B

Granular GMR materials: Fe/Cu, Fe-Ag, Co-Cu

(b) Quasi-granular films made by heat treating multilayers of immiscible solids

GMR films: $[Fe\text{-}Ni/Ag]_N$

(c) Nanograined layers grown on columnar films

Thin film magnetic recording media: Co-Cr-Ta/Co-Cr

(d) Columnar thin films and engineered nanowires

(e) Acicular particulate recording media : Cobalt-modified ferric oxide media: Co2+ γ-Fe_2O_3

(f) Four different types of thin-film structures whose unique properties arise from one nanoscale dimension :

Magnetic multilayers: $[Fe/Cr]_N$, Spin valves: Co/Cu/Ni-Fe, Spin switches: Ni-Fe/Cu/Ni-Fe

Spin-tunnel junction: F-I-F tunnel junctions such as $FeCo/Al_2O_3/Co$

(1) INTRODUCTION

▶ Key Factors understanding Magnetism of Nanostructured Materials

- Single-domain behavior

If the magnetostatic energy of the single-domain state is lower than the energy required for creating a domain wall, nanostructured materials should be composed of a single domain below a certain dimension.

- Superparamagnetism

Below a critical particle dimension, the remanent magnetization is no longer fixed in the direction dictated by particle shape or crystal anisotropy because of ambient thermal energy (a magnetic analog of Brownian motion) and the coercivity becomes zero because of thermal effects that are strong enough to spontaneously demagnetize particles. Typically below a radius of order 20 nm, magnetic particles become superparamagnetic.

- Exchange coupling: The coupling between spins on different sides of a physical interface

It is critical to understand the magnetic behavior of nanocrystalline materials and the behavior of many thin-film magnetic structures and devices). It is also the origin of the surface anisotropy.

- Random anisotropy: Local magnetic anisotropy in amorphous alloys and nanstructured materials

It is relevant in treating the variation in direction of magnetization from particle to particle.

- Surface anisotropy: The magnetic anisotropy at the film surface due to exchange coupling

It is different from the bulk anisotropy and important to thin-film magnetism.

(1) INTRODUCTION

Single–domain particles between r_o and r_c

$$r_c \approx 9\frac{(AKu)^{1/2}}{\mu_0 Ms^2} \quad \text{(strong anisotropy)}$$

$$r_c \approx \sqrt{9\frac{A}{\mu_0 Ms^2}\left[\ln\left(\frac{2r_c}{a}\right)-1\right]} \quad \text{(weak anisotropy)}$$ cf) $r_o^{1\,yr} = (9kT/K_u)^{1/3}$

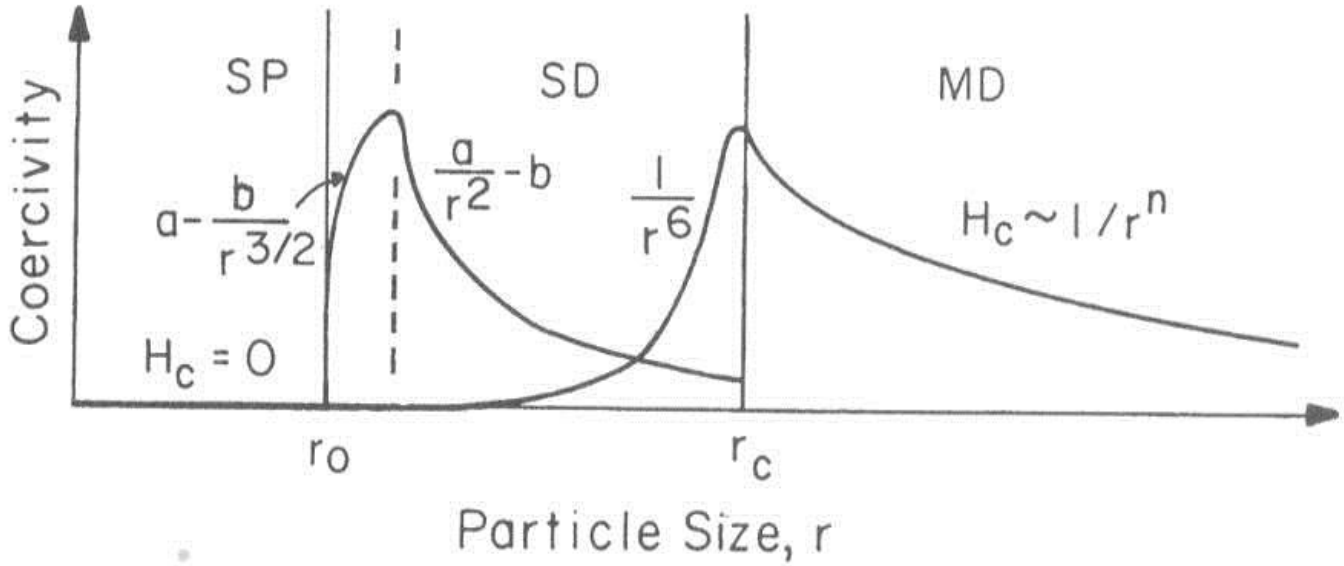

(1) INTRODUCTION

A critical film thickness, t_c below which the single-domain state is stable

The total energy density,

$$f_{total} = 2(1.7\sigma_{dw}\mu_o M_s^2 t)^{1/2}/L$$

Free energy of the single-domain state

$$f_{ms}^{sd} \approx \left(\frac{Wt}{L^2}\right)\left[\ln\left(\frac{4L}{W+t}\right)-1\right]\mu_0 M_s^2$$

Therefore,

$$t_c \approx 4\left(\frac{L}{W}\right)^2\left(\frac{1.7\sigma_{dw}}{\mu_0 M_s^2}\right)\left[\ln\left(\frac{4L}{W+t}\right)-1\right]^{-2}$$

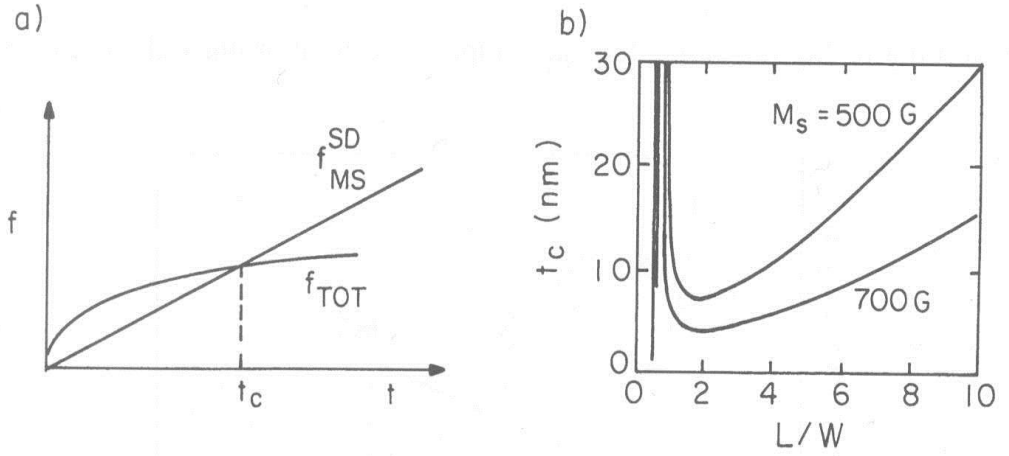

Figure 8.19 (*a*) Comparison of the thickness dependence of the free energy density for the demagnetized state f_{tot} [Eq. (8.23)] with the free energy density for the single domain state, f_{ms}^{sd} [Eq. (8.24)]. Note the crossover below which the energy is lower for the single-domain state. (*b*) Variation of the criticdal thickness with the ratio L/W for two different values of magnetization and $\sigma_{dw} = 0.1\ \text{mJ/m}^2$.

(2) Exchange Coupling

Exchange Coupling?

- **The coupling between spins on different sides of a physical interface, leading to a preferential relative orientation of two different magnetic materials**

- Different from a long-range magnetostatic dipole coupling at the boundary between two materials

- The spins in magnetic particles or layers of different materials can be coupled with different strengths or even different signs depending on the nature of their exchange interaction and the thickness and properties of the material between them

Types of exchange coupling

- **Ferromagnetic-Antiferromagnetic (F/A) Exchange Coupling**
- **Ferromagnetic-Ferromagnetic Coupling**
- **Oscillatory Exchange Coupling**

(2) Exchange Coupling

❑ Ferromagnetic-Antiferromagnetic (F/A) Exchange Coupling

M-H loops of fine Co particles ($2r \approx 20$ nm)

- Displacement of the field axis is due to the existence of a CoO thin surface layer

  CoO : paramagnetic above T_N (= -3 °C), antiferromagnetic below T_N

- Below T_N , Co moments in CoO are ferromagnetically coupled in {111} planes with the Co moments in adjacent {111}planes antiparallel.

- The magnetic moments in the CoO chose an axis of magnetization that minimizes their energy of interaction with the Co moment across the interface, leading to the field-displaced loop exhibiting ***exchange anisotropy***, which results from an ***exchange coupling*** between the moments of Co and CoO.

- Definition of the coercivity H_c and exchange field H_{ex}

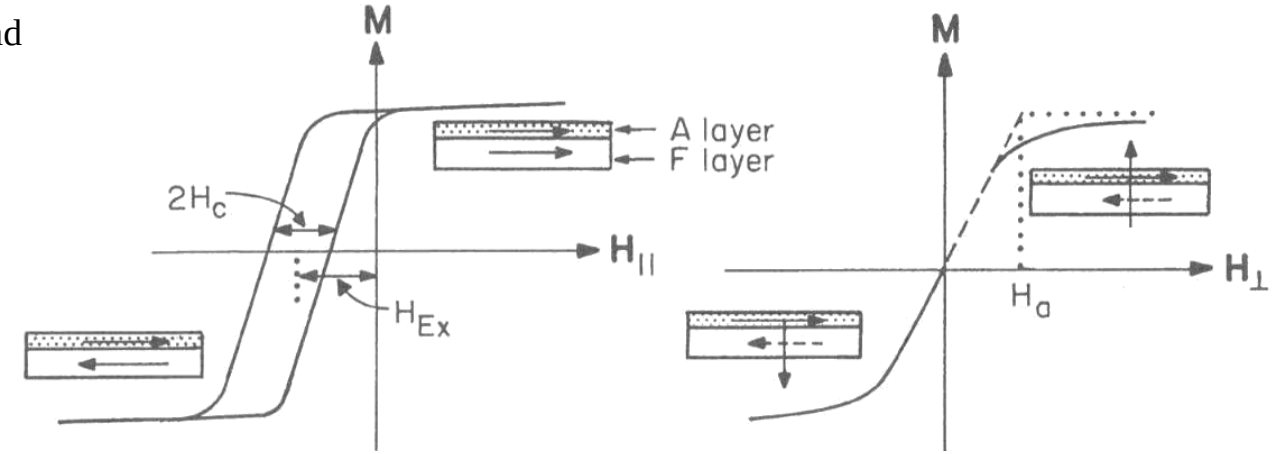

(2) Exchange Coupling

❑ Ferromagnetic-Antiferromagnetic (F/A) Exchange Coupling

M-H loops of fine Co particles ($2r \approx 20$ nm) (continued)

- A stronger negative field is required to demagnetize the sample than if it had been cooled in zero field. (Figs. in Cullity)

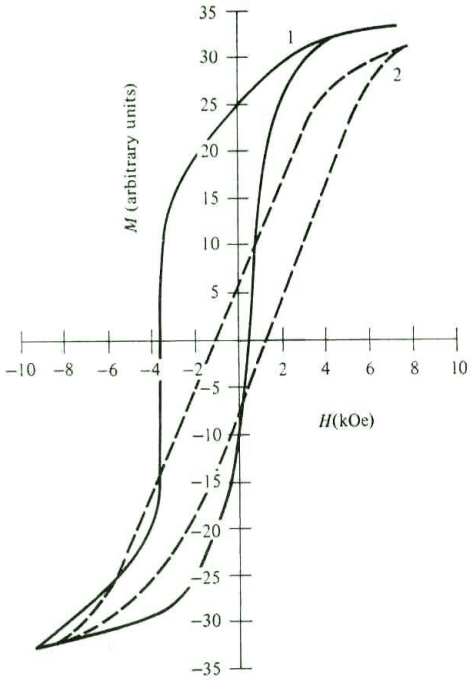

그림 11.25 77°K 에서 측정한 산화물이 피복된 코발트입자의 자기이력곡선. 루프(1)은 + 10KOe 의 자장하에서 냉각된 결과이며 (2)는 무자장하에서 냉각된 결과이다. Meiklejohn 과 Bean[11.28]

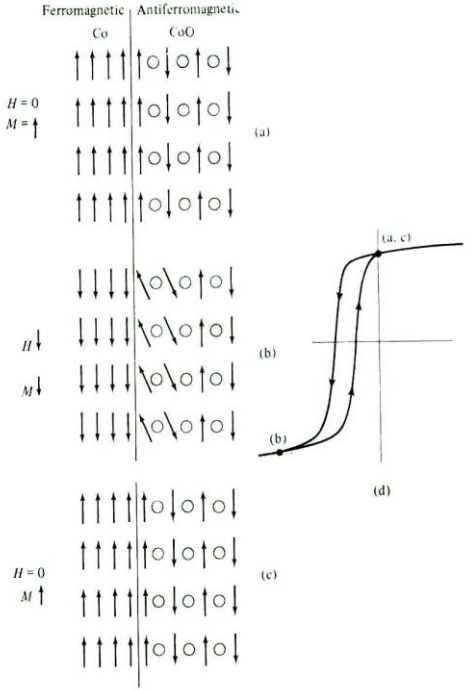

그림 11.27 Co−CoO 입자에서 루프가 이동하는 기구. 화살표는 코발트원자 또는 이온의 스핀을 표시하며 동그라미는 산소이온을 표시한다. 이력곡선에서의 (a), (b), (c)는 왼편의 3가지 상태에 해당되는 점이다. Graham[10.1]

(2) Exchange Coupling

Interpretation

The actual microscopic moment arrangement of F/A exchanged coupled materials

- Soft ferromagnetic layer exchange-coupled to an antiferromagnetic layer (see Fig. 12.4)

- The exchange coupling across the interface is such that the moments in the A material lie on an axis that is orthogonal to the F moment at the time of cooling through T_N, which is the lower energy configuration because it is easier to cant the A moments into the direction of an orthogonal field than one that is parallel to the preferred A axis.

- Why does the twist in magnetization occur mostly in the soft F layer?

i) a small magnetic anisotropy in the F layer

ii) no net torque on the A moments

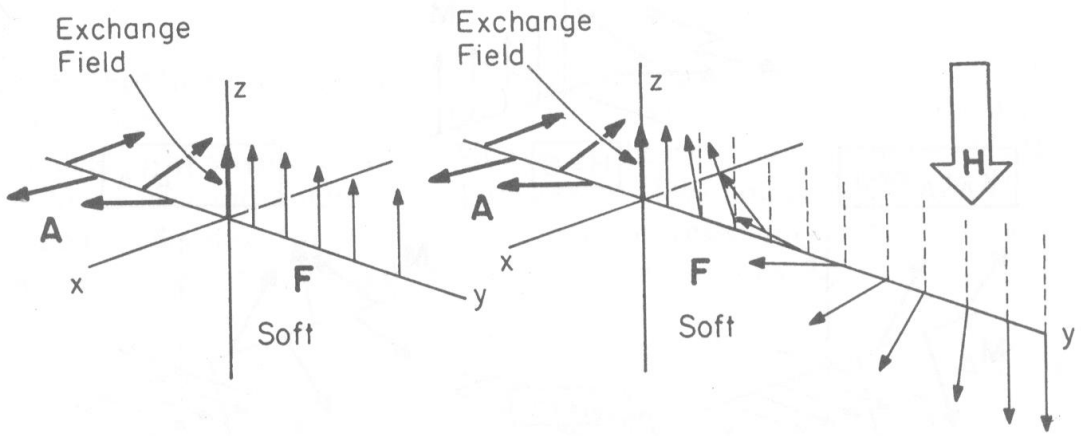

(2) Exchange Coupling

The actual microscopic moment arrangement of F/A exchanged coupled materials (continued)

- In the case that the thickness of the F material is less than the thickness of a domain wall or exchange length (see Fig. 12.5 in O'Handley) : no magnetization twist in F

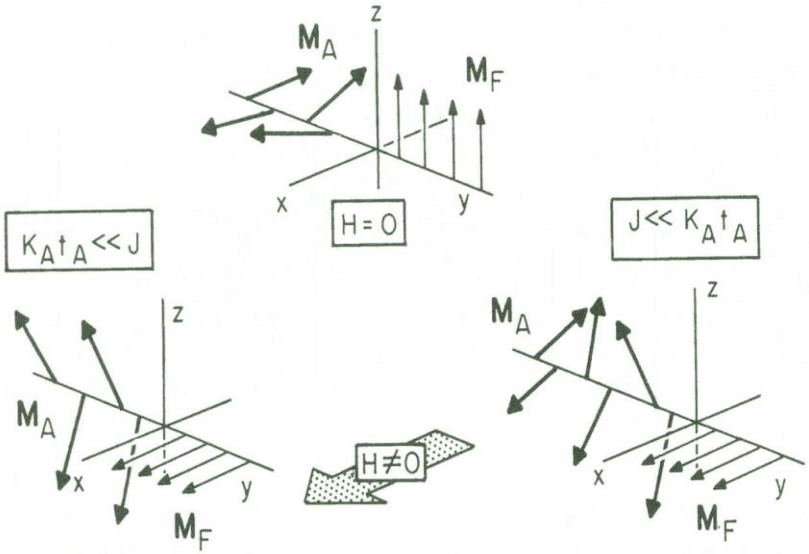

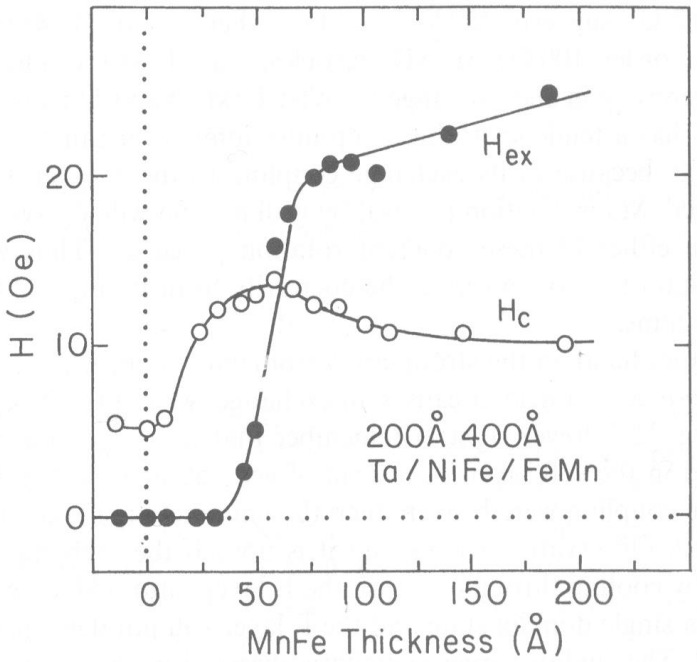

- If the A material were not sufficiently thick (see Fig. 12.6 in O'Handley)

(2) Exchange Coupling

In F/A exchanged coupled materials

- The exchange coupling (*i.e.*, exchange anisotropy) disappear below a certain thickness of the A material.

The condition for no exchange anisotropy

$$t_A \le \frac{J}{K_A} = t_A{}^c$$

Coercivity

For a weak-A

Coherent rotation of MF against its anisotropy KF

$$H_c \le 2\frac{K_F}{M_F}$$

Rotation of the MA against KA by the interface torque

$$H_c \le 2\frac{K_A t_A}{M_F t_F}$$

For a strong-A

$$H_c \le 2\frac{K_A \delta_A}{M_F t_F} \approx \frac{\sigma_{dw}^A}{2M_F t_F}$$

Exchange field

$$\frac{F}{Area} = -M_F H t_F \cos\theta + K_F t_F \cos^2\theta - J\sin\theta$$

$$\sin\theta[\cos\theta + \frac{M_F H}{2K_F} + \frac{J}{2K_F t_F}] = 0$$

$$H_{ex} = \frac{J}{M_s t_F}$$

Anisotropy field

$$\frac{F}{Area} = -M_F H t_F \cos\theta + K_F t_F \cos^2\theta - J\sin\theta$$

$$\cos\theta = m_x = \frac{M_F t_F}{2K_F t_F + J} H \equiv \frac{H}{H_a}$$

$$H_a = \frac{2K_F t_F + J}{M_F t_F} = H_{a0+} \frac{J}{M_F t_F}$$

(2) Exchange Coupling

In F/A exchanged coupled materials (continued)

- Exchange field and coercivity versus NiFe thickness (see Fig. 12.7 in O'Handley) $H_c, H_{ex}, H_a \propto t_F^{-1}$

- Anisotropy, exchange and coercivity fields versus permalloy thickness (see Fig. 12.8 in O'Handley)

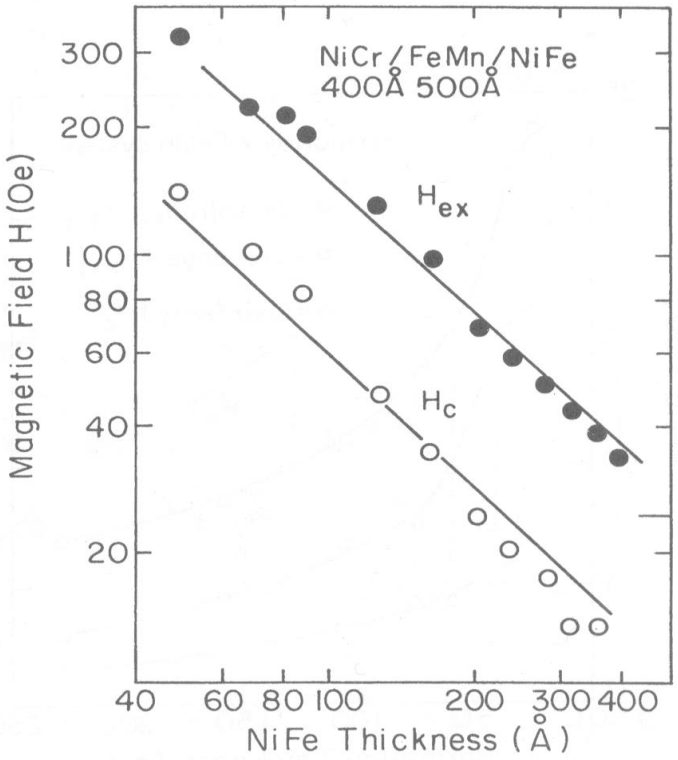

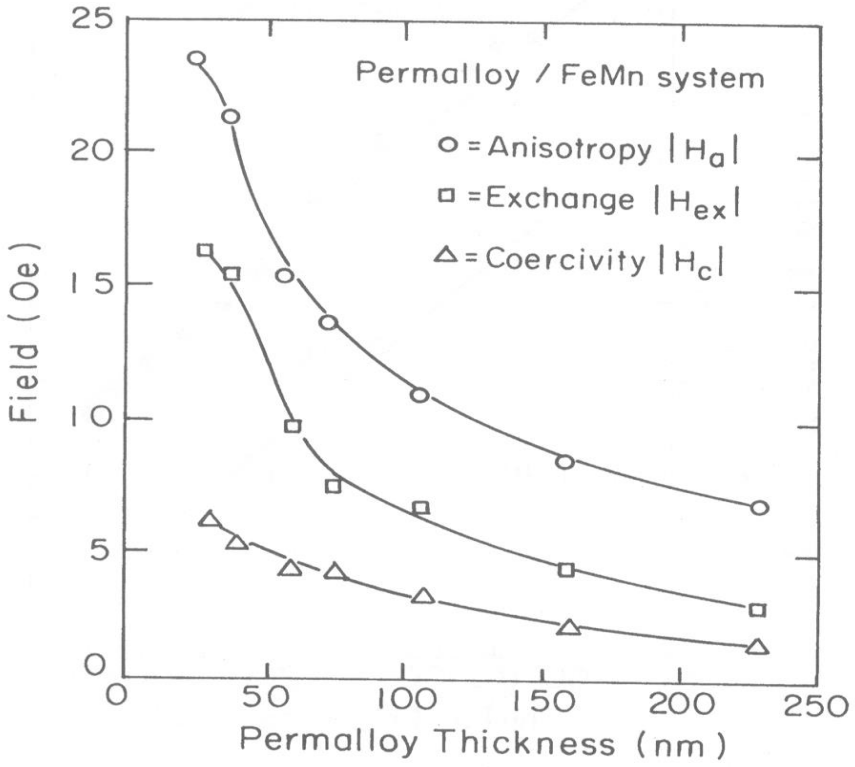

(2) Exchange Coupling

A complementary microscopic model that addresses the strength of J from a statistical perspective

$$H_{ex} = \frac{j_{ex} S_F \cdot S_A}{a^2 M_s t_F}$$

Assuming Heisenberg exchange across an atomically smooth F/A interface

(See Fig. 12.11 and Fig. 12.12 in O'Handley)

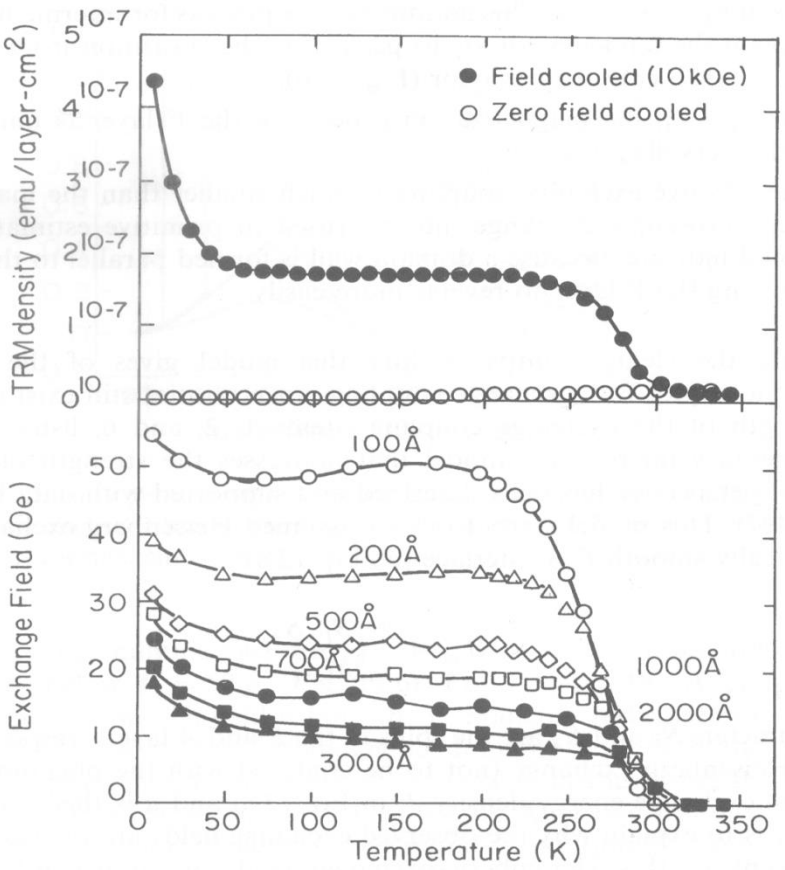

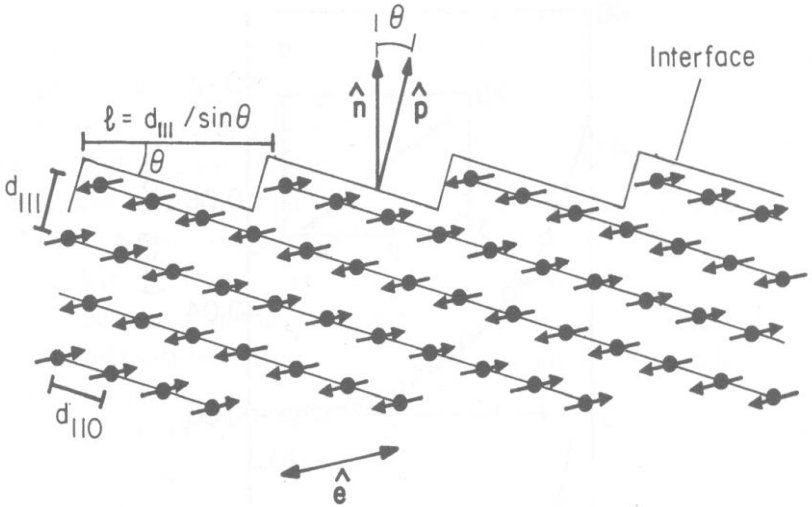

(2) Exchange Coupling

Examples of F-A exchange coupling across a nonmagnetic layer (see Fig. 12.13 in O'Handley)

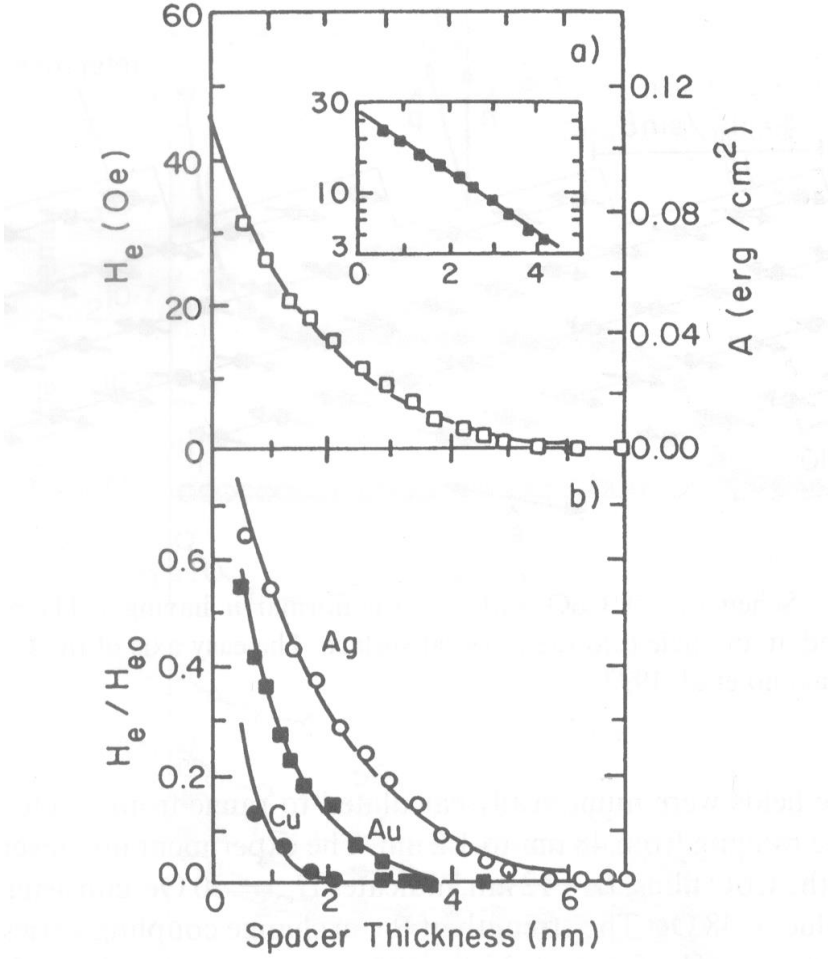

(2) Exchange Coupling

❑ Ferromagnetic-Ferromagnetic Exchange Coupling

Origins: a direct Heisenberg-like exchange interaction or an indirect RKKY-like exchange interaction

- When the magnetization at the interface has no perpendicular component:

$$M_{//}\text{ (parallel to interface)} : l_{ex}^{\parallel(i)} = (A^{(i)}/K_u^{(i)})^{1/2} \quad i = \text{medium 1, 2}$$

The spin orientation at the interface will be biased toward that of the stronger anisotropy material.

- When there is a perpendicular component of magnetization at the interface

$$M_{\perp}\text{ (perpendicular to interface)} : \quad l_{ex}^{\perp(i)} = \{A^{(i)}/(K_u^{(i)} + 2\pi \triangle M_{\perp}^{2})\}^{1/2}$$

The exchange interaction through the parameter l_{ex}, has the effect of communicating the magnetization direction in one region over distances of several nanometers into another, exchange-coupled region.

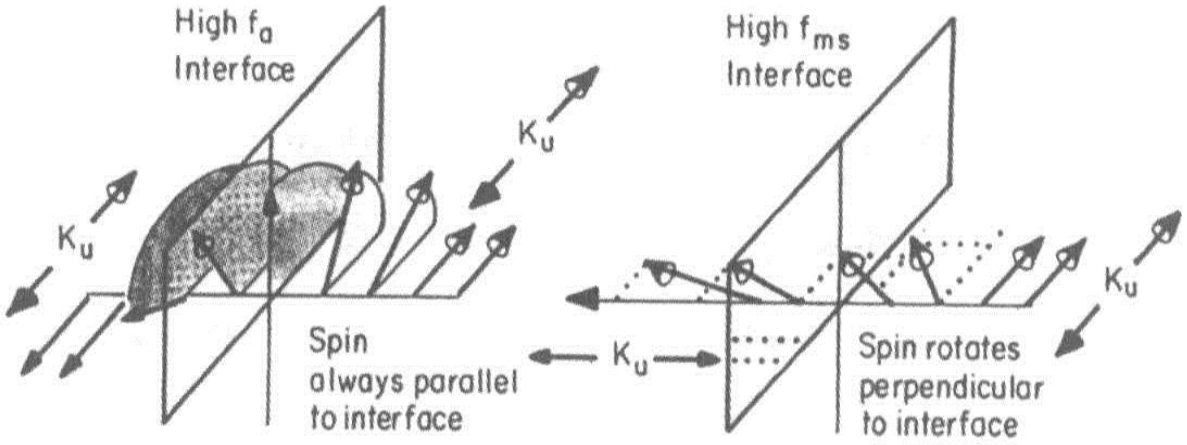

(2) Exchange Coupling

❑ Ferromagnetic-Ferromagnetic Exchange Coupling (참고)

Domain Walls near Interfaces: The Exchange Length, l_{ex}

The exchange length l_{ex} (or pinned wall thickness) : the thickness of the magnetization orientation transition when the magnetization is pinned in a direction different from the easy axis in the interior of the material

- Two cases

(i) No perpendicular magnetization component near the interface

M rotation is driven toward the easy axis by the interior anisotropy energy.

$M_{//}$(parallel to interface) : $l_{ex}^{\parallel} = (A/K_u)^{1/2} = \delta_{dw}/\pi$

(ii) Non-zero perpendicular magnetization component near the interface ***M*** rotation is driven toward the easy axis by both the interior anisotropy energy and the magnetostatic energy associated with the charged interface.

$M_{\perp}$(perpendicular to interface) :

$$l_{ex}^{\parallel} = \{A/(K_u + 2\pi \triangle M_{\perp}^{2})\}^{1/2}$$

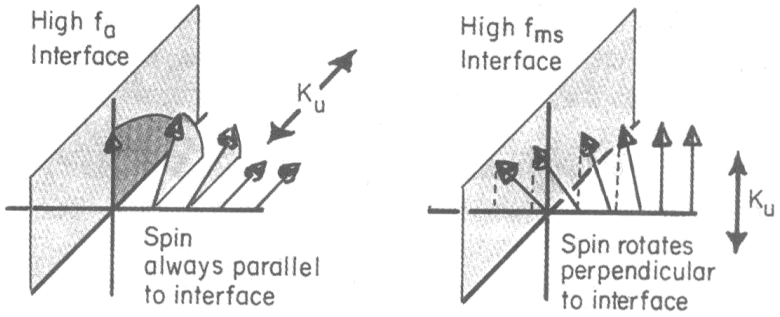

Figure 8.15 Illustration of the two cases important for determining the range of the twist in magnetization on moving from an interface at which the spins are pinned in a direction different from the interior of a ferromagnetic material. At left, the surface pinning holds the magnetization in the plane of the interface so magnetostatic energy is not an issue. At right, the surface spin pinning is such that a perpendicular component of magnetization exists near the interface. The magnetic charge at the interface gives rise to a local magnetostatic field that tends to shorten the exchange length.

(2) Exchange Coupling

❑ **Oscillatory Exchange Coupling:** A long-range oscillation exchange coupling

Physical mechanism: Long-range oscillation in exchange coupling in two-dimensional magnetic nanostructures is believed to be related to *the spin polarization of conduction electrons* as described by the RKKY model.

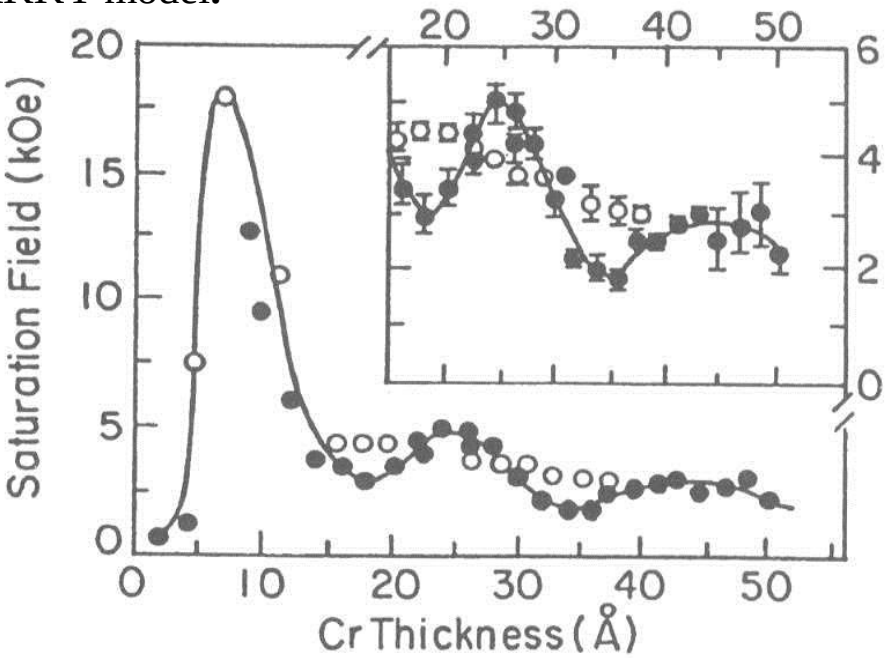

Saturation field of $[Fe/Cr]_N$ multilayers along a hard <110> in-plane direction at 4.2 K vs Cr thickness for Si(111)/100Å Cr/[20Å Fe/t_{Cr}Cr]$_N$/50Å Cr, open circle and square : N = 30, deposited at 40°C, closed circle and square : N =20°C, deposited at 125°C

Key points :

- Large saturation fields at 10, 24, 45 Å of Cr : strong antiferromagnetic coupling between the Fe (or Co) layers
- Small saturation fields : ferromagnetic coupling between the Fe layers
- $[Co/Cu]_N$ multilayers : an exchange coupling of the Co layers that oscillates from antiferromagnetic to ferromagnetic as t_{Cu} increases
- Typical oscillation period ~ 1 nm, spacer thickness ~ 5-6 nm

(2) Exchange Coupling

❑ Oscillatory Exchange Coupling (continued)

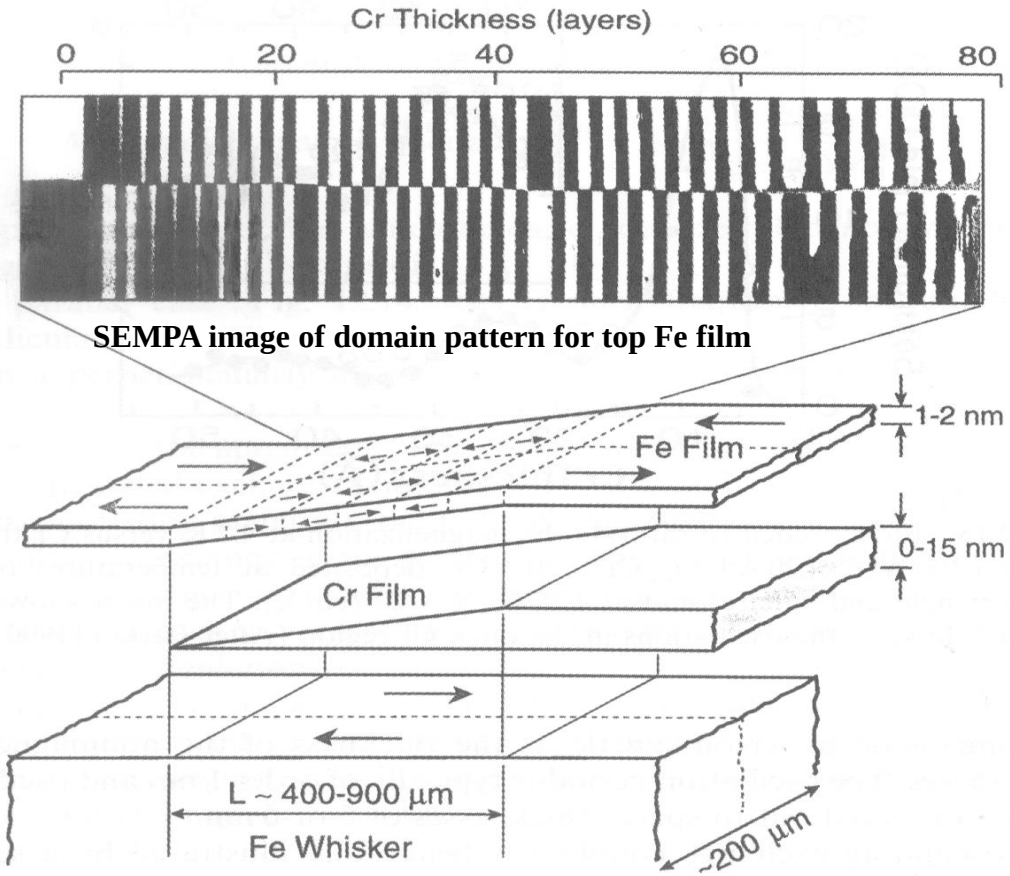

SEMPA image of domain pattern for top Fe film

Structure of Fe film/Cr wedge/Fe whisker illustrating the Cr thickness dependence of FeFe exchange

Key points :

- The Fe film is exchange coupled through the Cr layer to the magnetization in the whisker below.

- As t_{Cr} increases, the exchange coupling is directly observed to oscillate to antiferromagnetic and back to ferromagnetic with a period corresponding to Cr atomic layers.

- No oscillatory exchange coupling was observed in F/A exchange coupling

(2) Exchange Coupling

❑ Random Anisotropy in Nanostructured Materials

- Randomly oriented local magnetic anisotropy in amorphous alloys and nanostructured materials

- Origin : Local crystal field giving rise to a local magnetocrystalline anisotropy, K_{loc}
- In amorphous alloys, the orientation and strength of this local anisotropy varies with position.
  (see Fig. 11.11 in O'Handley)

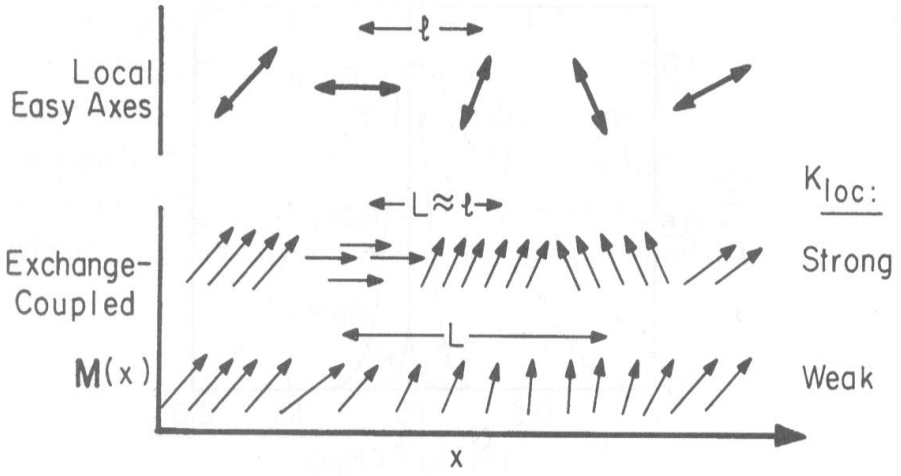

Figure 11.11 Schematic representation of the variation of local anisotropy easy axis with position and the variation of magnetization direction in response to the local anisotropy and exchange coupling. $M(x)$ closely follows a strong local anisotropy and is a smoother function of x for weak local anisotropy.

(2) Exchange Coupling

❑ Random Anisotropy in Nanostructured Materials (continued)

- When interparticle exchange and random anisotropy combine to affect the magnetic properties of discrete magnetic systems such as nanocrystalline alloys,

Two important effects

(i) The magnetization experiences an anisotropy reduced from its local value K_{loc} by exchange-averaging over the random local anisotropy : $\langle K \rangle \approx K_{loc}(l/L)^{3/2}$
(see Fig. 11.11 in O'Handley)

(ii) The magnetization shows an orientational coherence over a length, $L = l_{ex}$: $L \approx l_{ex} = 16A^2/9K_{loc}{}^2 l^3$
(see Fig. 12.17 in O'Handley)

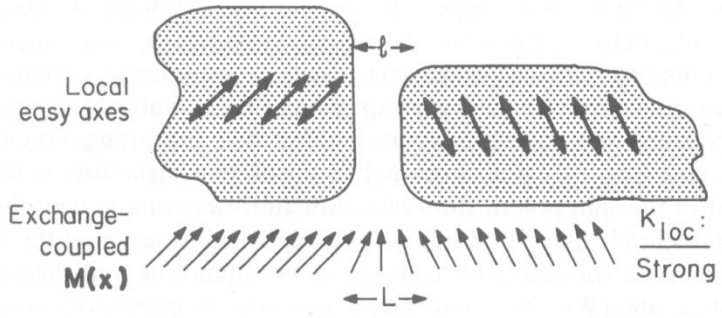

The appropriate length scale l for the random anisotropy magnetization direction is given by the thickness of the interparticle layer.

Suggestion by Herzer (1993)

From $l_{ex}^{(i)} = [A^{(i)}/K_u^{(i)}]^{1/2}$ and $l_{ex} = 16A^2/9K_{loc}{}^2 l^3$

$\langle K \rangle \approx 0.32(K_u^4/A^3)l^6$: explainable for a steep rise in H_c in nanostructured system
(see Fig. 9.19 in O'Handley)

(3) Nanostructured Magnetic Materials

❑ Processing

Bulk specimens:
- Quenching certain alloy compositions from the melt
- Heat-treatment of an amorphous alloy precursor
- Addition of nucleation centers or grain growth inhibitors

Films:
- Fabrication of two-dimensional films and multilayers: Sputtering, Electrodeposition, MOCVD, E-beam evaporation/condensation

❑ Examples

- **The Co-Nb-B system** (Fig. 9.19 in O'Handley)
  Annealing of amorphous Co-Nb-B
  Hc depends on the size of nanocrystallites
  AC loss greatly decreases with decreasing the size

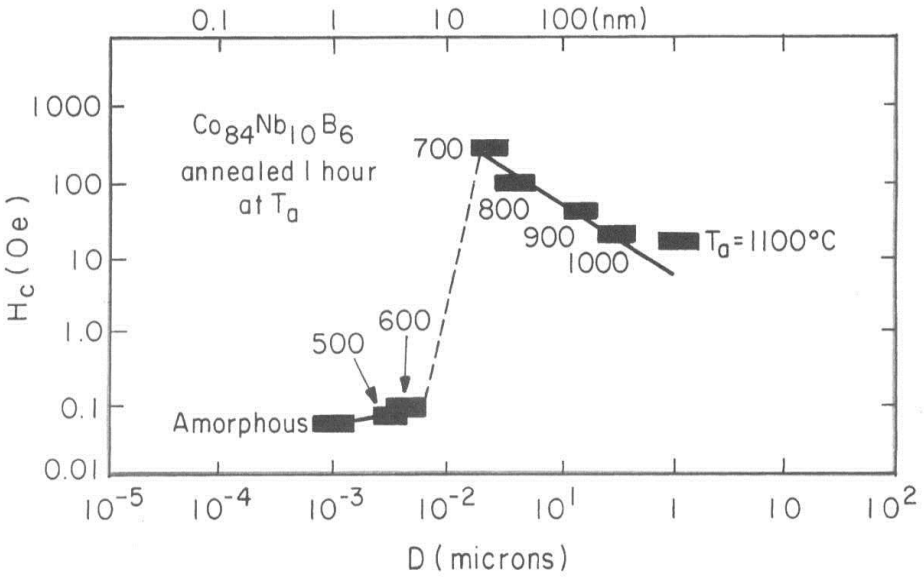

Variation of coercivity in amorphous and crystallized CoNbB as a function of mean particle size. Average D of nanocrystallites was determined by TEM.

(3) Nanostructured Magnetic Materials

- **The Fe-B-Si-Nb-Cu system** (Figs. 12.18-19 in O'Handley)

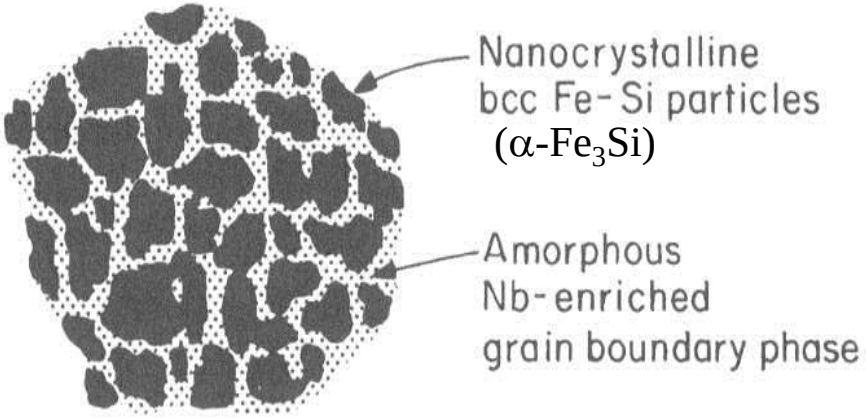

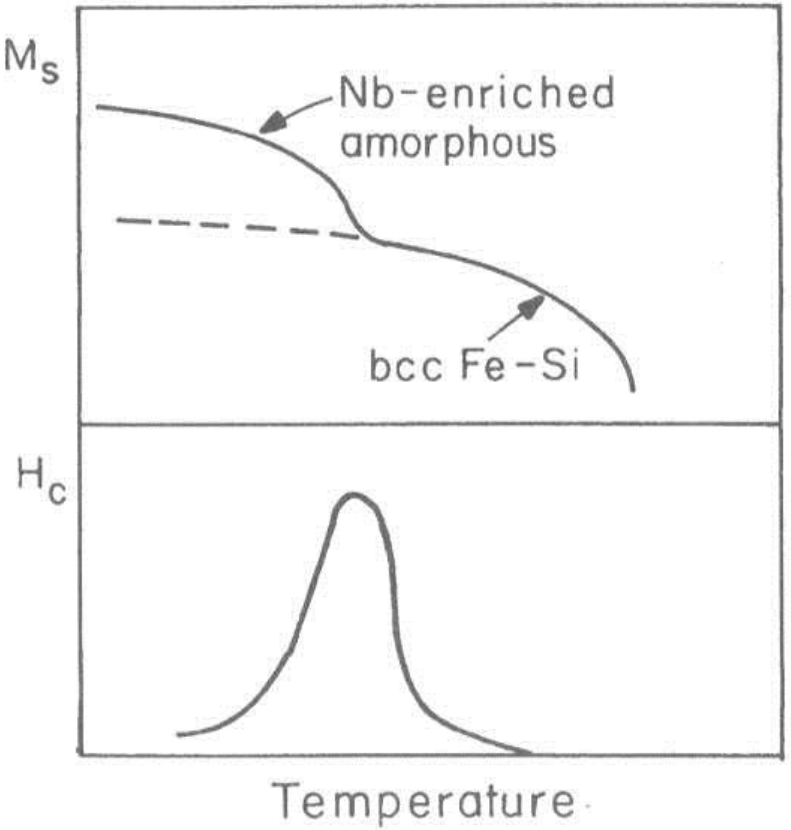

- SD α-Fe_3Si particles : exchange coupled for T < Tc (amorphous)
  decoupled for T > Tc (amorphous)
- Origin of the peak in Hc at the decoupling temperature :
  No longer switch in unison for the entire magnetization cycle as the exchange coupling weakens (See Fig. 12.6 in O'Handley)
- Hc $\rightarrow$ 0 for Tc(amorphous) < T < Tc (α-Fe_3Si) :
  Superparamagnetic behavior of SD α-Fe_3Si particles

(3) Nanostructured Magnetic Materials

- **$(Fe,Co)_{81}M_9C_{10}$(M= Ta, Hf, Zr, Nb,...)** (Figs. 12.20-24 in O'Handley)

Inclusion of refractory metals : Increase in the strength, stability, and corrosion resistance of alloys

Annealing of metastable amorphous transition metal carbon alloys

Grain size of α–FeCo : 5-10 nm

Grain size of M carbide nanocrystals (stable grain boundary phase) : 1-4 nm

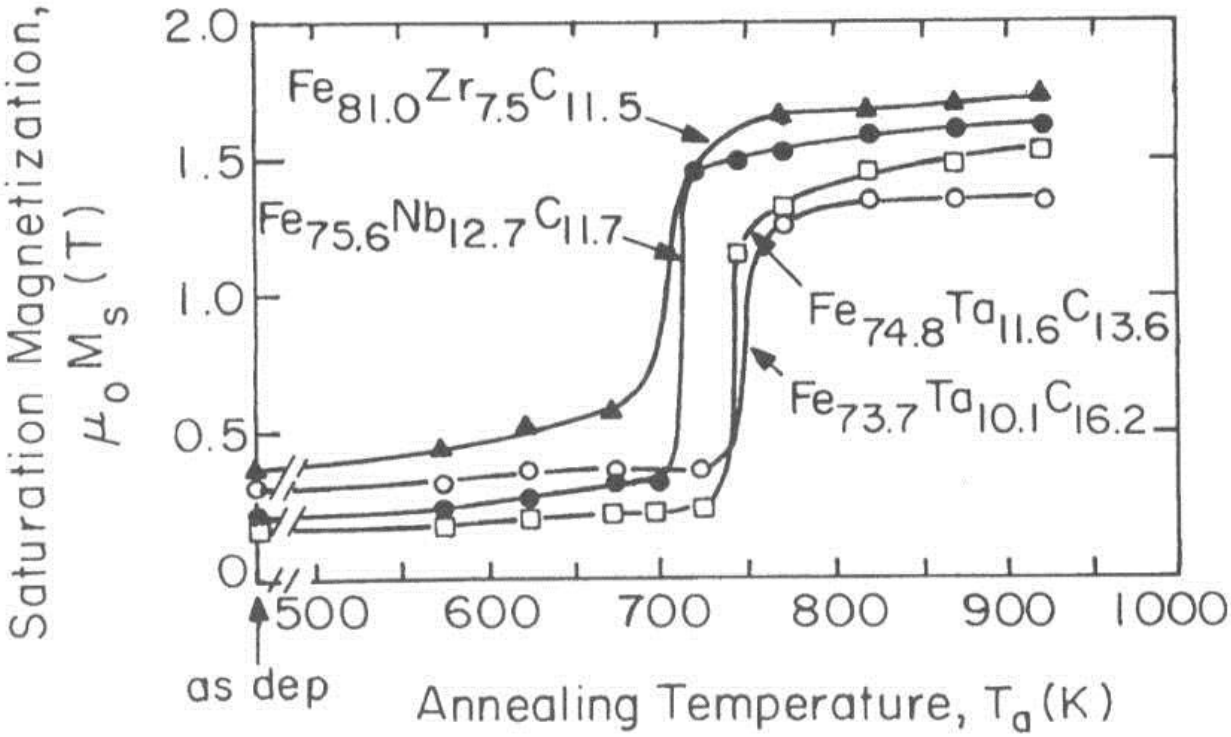

(3) Nanostructured Magnetic Materials

- **CoCrTa-(Pt) Recording Media** (Figs. 12.25 in O'Handley)

  CoCr alloys :

  - HCP phase below 18% Cr exhibiting strong magnetic anisotropy with high Hc
  - Important in magnetic recording media
  - Ta or Pt addition retard grain growth and promote segregation of nonmagnetic refractory metals and oxides to the grain boundaries.

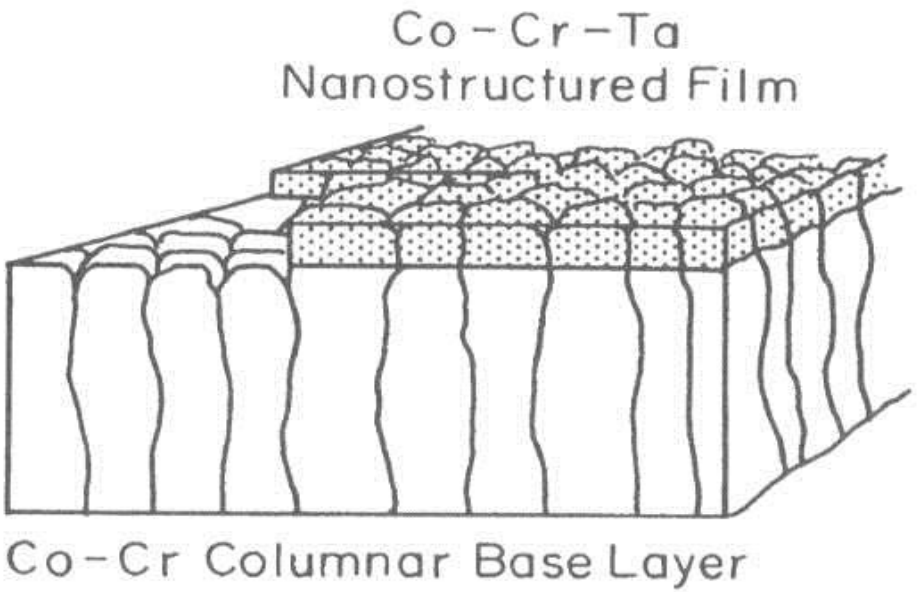

(3) Nanostructured Magnetic Materials

- **Nanostructured Permanent Magnets** (Figs. 12.26-28 in O'Handley)

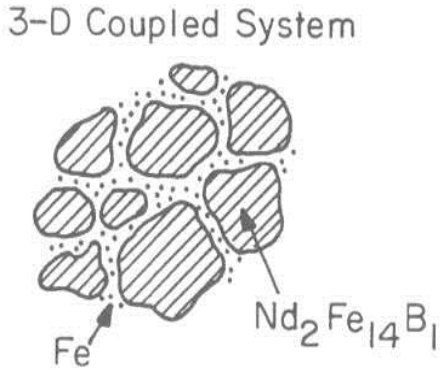

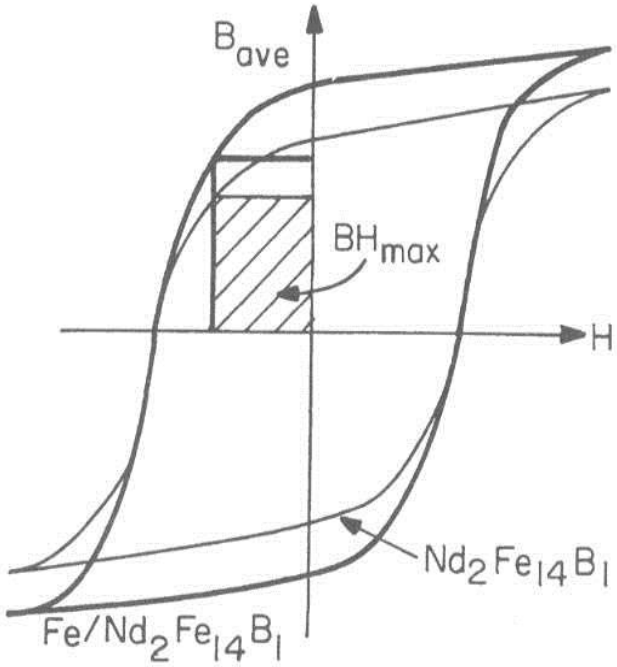

Improvement in Br by exchange-coupling the high-anisotropy $Nd_2Fe_{14}B_1$ grains (20-40 nm) to a larger magnetization α-Fe (5-10 nm) intergrannular phase.

Pure 2-14-1 : Br =16 kG

iHc > 20 kOe

- **Nanotubes and Nanowires** (Fig. 12.1 in O'Handley)